MODELLING AND CONTROL OF SEVEN DOF RIDE MODEL USING HYBRID CONTROLLER OPTIMIZED BY PARTICLE SWARM OPTIMIZATION

M. H. I. M. Amin[1*], K. Hudha[2], N. H. Amer[3],
Z. Abd Kadir[4], A. Faiz[5]

[1,2,3,4] Department of Mechanical Engineering, Faculty of Engineering,
Universiti Pertahanan Nasional Malaysia, Kem Sungai Besi, 57000 Kuala Lumpur, Malaysia.

[5] Department of Electrical Engineering, Faculty of Electrical Engineering,
Universiti Teknologi MARA, 81750 Pasir Gudang, Malaysia

ABSTRACT

In this study, a seven degree of freedom (DOF) ride model of armored vehicle is employed in control system to control the vehicle ride performance especially in body acceleration, body pitch acceleration and body roll acceleration due to extreme road profile and disturbance using Hybrid control structure optimized by Particle Swarm Optimization (PSO) algorithm. The seven DOF ride model parameters are obtained from CARSIM software by selecting heavy vehicle High Mobility Multipurpose Wheeled Vehicle (HMMWV) as a benchmark. The performance of the hybrid control structure without optimization was compared to the performance of a simple PID control structure and passive seven DOF vehicle ride model. Lastly, the performance of Hybrid control structure without optimization were compared to the performance of Hybrid control structure optimized by PSO algorithm.

KEYWORDS: *Seven DOF; HMMWV; PSO; hybrid; skyhook; PID; semi-active suspension; passive suspension*

1.0 INTRODUCTION

Armored vehicles have been a key weapon in ground battlefield due to its excellent operational mobility, tactical offensive and defensive capabilities (Dhir & Sankar, 1997). In addition, the armored vehicle is designed to operate on extreme conditions and it has a long firing system beneficial in an enemy attack. In recent technologies, armored vehicles are equipped with numerous safety systems to enhance the ride and handling performance in various conditions, especially during combat. There are two types of the armored vehicle system which is wheeled and tracked by the equipped suspension system (Chen, Wang, Qiu & Huang, 2012). For military applications, wheeled and tracked armored vehicles are designed to operate in rough road terrain, which emphasize the importance of a well-designed suspension system (Uddin, 2009). The

* Corresponding Email: mhafizikhwan91@gmail.com

function of the suspension system is to maintain the comfort level of soldiers travelling in the armored vehicle and to minimize the components damage during maneuver (Dhir & Sankar, 1997).

As the operating speed of high mobility wheel armored vehicle increases, the vibration induced by extreme road condition will also increase (Chen et al., 2012). This will reduce the comfort level, stability and ride performance of the armored vehicle. Therefore, it will induce fatigue to the soldier members that are travelling in that armored vehicle and damage the components installed inside. Besides that, excessive vibration in armored vehicles limits the maximum vehicle speed. Hence, the percentage of survivability and operational efficiency in battlefield situations will also reduce. One of the methods to enhance the ride performance and safety of the high mobility wheeled armored vehicle is by improving the performance of suspension system due to the road excitations in the vertical direction of the armored vehicle. The suspension system has become one of the major considerations to enhance ride and handling performances of armored vehicles according to previous works (Trikande, Jagirdar, & Sujithkumar, 2014).

The main function of the armored vehicle suspension is to isolate the passenger compartment from the road vibration to increase the comfort level. According to Liang and Wu (2013), the conventional passive suspension accomplishes this by supporting the passenger compartment with spring. Theoretically, as the spring rate reduced, the ride quality of sprung mass increased. However, this situation will increase the roll moment acting on an armored vehicle during cornering. A higher stiffness spring is required to reduce roll moment during cornering. Subsequently, a passive suspension results in a conflict between ride comfort and handling of the armored vehicles. Another function of a suspension system is to maintain contact between the tires and the road surface in order to provide steering stability for good handling performance and ensuring the comfort of the passengers (Hayes, Beno, Weeks, Guenin, Mock, Worthington, & Lippert, 2015). A good armored vehicle equipped with the best suspension system to provide safety and increase the comfort level of the passenger. According to Bakar, Jamaluddin, Rahman, Samin and Hudha (2008), the outstanding performances of ride comfort and operational stability can be observed during acceleration and braking condition of armored vehicles.

There are three types of suspensions system generally studied by researchers namely passive, active and semi active suspension. The conventional passive suspension system has the ability to store energy via a spring during compression stage and dissipates it via a damper during extension stage of suspension system (Hudha, Jamaluddin, Samin, & Rahman 2005). In real automotive application, the passive suspension system is chosen in order to achieve a certain level of road holding, load carrying, ride comfort and performance by tuning fixed parameters for spring and damper. Meanwhile, the semi active suspension system functions as passive suspension system, but it uses variable damper with varying damping coefficient of suspension to cater various disturbance in road condition. The active suspension system has the ability to store, dissipate and create new energy within suspension system by the helps of an actuator (Bakar et al., 2008). An advanced controllable suspension system such as semi active and active suspension system can produce better performance in order to improve the ride quality of an armored vehicles compared to the conventional passive suspension system. In addition, the characteristic of active and semi active suspension systems possess variable parameters thus enables the suspension to be highly robust and adjustable depending on the road conditions experienced by armored vehicles.

Previously, active suspension system has been studied by other researchers for the tracked and wheeled armored vehicle. Weeks, Bresie, Beno & Guenin (1999) proposed a combination of a fully controlled electromechanical actuator and passive spring to stabilize vehicle dynamics and improve the efficiency of an armored vehicle static weight support. Besides that, Liang et al. (2013) developed an active suspension system utilizing a low cost, high performance switch reluctance actuator with linear matrix inequality optimization method by using LQG- Based Fuzzy Logic controller to enhance the ride performance of armored vehicle. Meanwhile, Hudha et al., (2008) focused on 12 DOF vehicle model to study the active suspension with Stability Augmentation System (SAS) to improve the dynamic performance of the light armored vehicle compared to the passive suspension system. In addition, stochastic optimal preview control was studied by Uddin (2009) for the active suspension system of a full vehicle model.

Meanwhile, some researchers such as Hosseinloo, Vahdati and Yap (1993) and Hoogterp, Saxon and Schihl (1993) had developed an on-off semi active suspension system based on 3 DOF model for a tracked armored vehicles to improve ride comfort characteristics. Miller and Nobles (1988) proposed a semi active control system applied to M551 tank. The semi active control provides control effort by an active damper which consumes virtually no power compared to fully suspension system by an appropriate control algorithm. The semi active suspension system can achieve dynamic control which approaches that of an active suspension. In addition, four-wheels armored vehicles with semi active suspension system has been designed by modelling a High Mobility Multipurpose Wheeled vehicle (HMMWV) to control the response during and after firing for improvement of safety and ride performance (Hosseinloo et al., 1993). On the other hand, a semi active suspension system for an 8x8 armored vehicles with an On-Off Fuzzy Logic control strategy, Skyhook control and continuous Skyhook were proposed by Trikande et al. (2014) to reduce the unwanted sprung mass motion such as heave, pitch moment and roll moment during maneuvering.

The existing passive suspension system installed on a high mobility wheel armored vehicle is not suitable due to its system disadvantages. Armored vehicles are commonly associated with extreme terrain condition. Generally, the spring and damper stiffness of passive suspension system is constant. Hence, it shows a good ride performance for on-road condition only. However for the off-road condition, the suspension system could not vary its damping coefficient with the extreme road profile. That is why passive suspension system is not suitable for armored vehicles. To overcome this, active or semi active suspension can be proposed. Semi active suspension system was proven to produce almost the same outcome and performance achievable with the current suspension system (Setiawan, Safarudin & Singh 2009). Besides, semi active suspension system costs less than an active suspension system and easier to install in real life application than active suspension system. Therefore, this paper focuses on developing a control strategy for semi active suspension system using hybrid control strategy that involves PID controller and Skyhook controller. The control structure is developed using seven DOF vehicle ride model to study the ride performance of an armored vehicle. Last but not least, the hybrid control strategy for semi active suspension system will be optimized by Particle Swarm Optimization (PSO) algorithm to enhance the ride performance of armored vehicles.

2.0 VEHICLE MODELLING

In this study, High Mobility Multipurpose Wheeled Vehicle (HMMWV) as shown in Figure 1 is used as a reference to study the performance of body acceleration, body pitch acceleration and body pitch acceleration due to extreme road profile and disturbance.

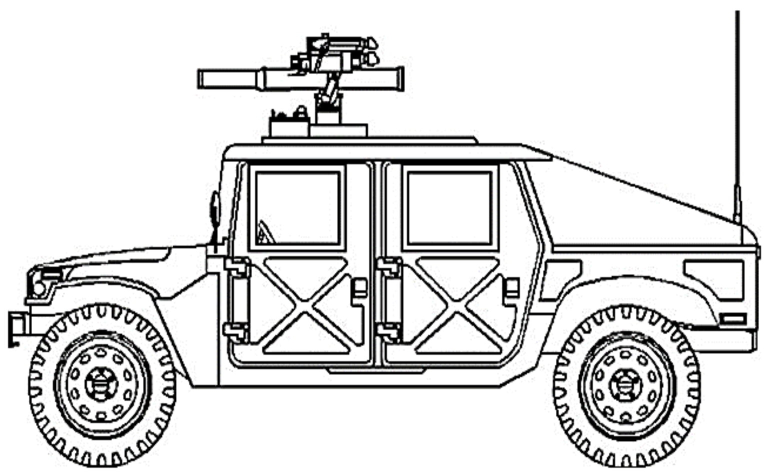

Figure 1. High Mobility Multipurpose Wheeled Vehicle (HMMWV)

2.1 Seven DOF Ride Model

The seven degree of freedom (DOF) ride model of High Mobility Multipurpose Wheeled Vehicle (HMMWV) is considered in this study. This vehicle model consists of a single sprung mass which is vehicle body that is connected to four unsprung masses (wheels) which is front right, front left, rear right and rear left located at each corner of the vehicle body. The sprung mass is allowed to have pitch and roll motions while the unsprung mass are allowed to bounce vertically with respect to unsprung mass (Setiawan et al., 2009). For each wheel, the passive suspension system between the sprung and unsprung mass were modeled schematically by a spring element and a passive damper. The wheels stiffness were assumed as a linear spring without damping (Ahmad, Hudha & Jamaluddin, 2010). This seven DOF ride model of HMMWV has been verified in the previous study (Amin et al., 2015).

From Figure 2, by utilizing this model, few assumptions were made. The vehicle body of seven DOF ride model is considered as a single lumped mass which is defined as sprung mass. While the drag force is ignored, the roll centre is aligned at the same level as the pitch centre and both are located at the centre of gravity (CG) of the armored vehicle; the suspension system between sprung mass and unsprung mass on each four corners of the vehicle are considered as passive dampers and spring element with constant damping coefficient and spring stiffness; and lastly, pitch and roll angle are neglected due to significantly small value (Ahmad et al., 2010).

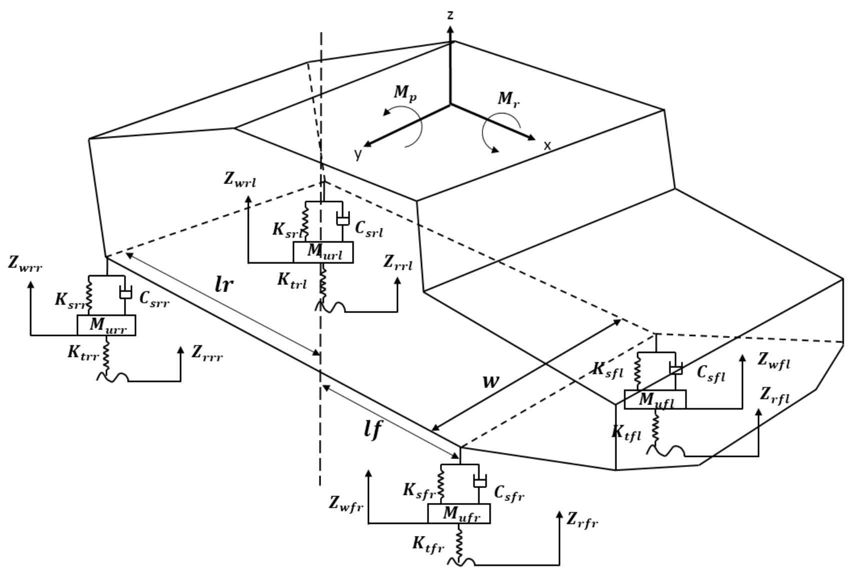

Figure 2. Seven DOF ride vehicle model

From Figure 2, equation of motion considering forces acting on sprung mass is given as;

$$F_{sfl} + F_{dfl} + F_{sfr} + F_{dfr} + F_{srl} + F_{drl} + F_{srr} + F_{drr} = M_s \ddot{Z}_s \tag{1}$$

where,

F_{sfl} = force of spring at left front side

F_{dfl} = force of damper at left front side

F_{sfr} = force of spring at right front side

F_{dfr} = force of damper at right front side

F_{srl} = force of spring at rear left side

F_{drl} = force of damper at rear left side

F_{srr} = force of spring at right rear side

F_{drr} = force of damper at rear right side

M_s = weight of sprung mass
$\ddot{Z}_s$ = acceleration of sprung mass at the CG

Meanwhile, road excitation and maneuvering tend to produce roll motion where the left and right suspension is being compressed and decompressed alternately. Same as pitch, the roll moment exists due to force produced at the CG of the armored vehicles in x-axis. The roll moment for the armored vehicle body is computed based on Newton's second law which is considering moments about axes on CG yields the equations for β and θ:

$$(F_{srl} + F_{drl} + F_{srr} + F_{drr})l_r - (F_{sfl} + F_{dfl} + F_{sfr} + F_{dfr})l_f = I_{\ddot{p}}\ddot{\theta} \quad (2)$$

$$(F_{sfl} + F_{dfl} + F_{srl} + F_{drl})\frac{w}{2} - (F_{sfr} + F_{dfr} + F_{srr} + F_{drr})\frac{w}{2} = I_r\ddot{\varphi} \quad (3)$$

where,

l_r = length between rear unsprung masses and centre of gravity
l_f = length between front unsprung masses and centre of gravity
$I_{\ddot{p}}$ = pitch axis moment of inertia
$\ddot{\theta}$ = pitch acceleration at body centre of gravity
w = wheel base
I_r = roll axis moment of inertia
$\ddot{\varphi}$ = roll acceleration at sprung mass CG

Other four DOF of the model consist of forces acted on each body of wheels that attached to the vehicle body. The suspension and tire forces at vertically exerted to the wheel during moving or in static condition. All the forces is derived based on basic equation of motion for the unsprung masses at each corner of sprung mass can be defined as;

$$F_{tfl} - F_{sfl} - F_{dfl} = m_{zfl}\ddot{Z}_{wfl} \quad (4)$$

$$F_{tfr} - F_{sfr} - F_{dfr} = m_{zfr}\ddot{Z}_{wfr} \quad (5)$$

$$F_{trl} - F_{srl} - F_{drl} = m_{zrl}\ddot{Z}_{wrl} \quad (6)$$

$$F_{trr} - F_{srr} - F_{drr} = m_{zrr}\ddot{Z}_{wrr} \quad (7)$$

where,

$F_{tfl}, F_{tfr}, F_{trl}, F_{trr}$ = tire force (left front, right front, left rear, right rear)
$m_{wfl}, m_{wfr}, m_{wrl}, m_{wrr}$ = unsprung mass (left front, right front, left rear, right rear)
$\ddot{Z}_{wfl}, \ddot{Z}_{wfr}, \ddot{Z}_{wrl}, \ddot{Z}_{wrr}$ = unsprung mass acceleration (left front, right front, left rear, right rear)

2.2 Development of Control Strategy for Semi Active Suspension System

Control structure proposed in this study consists of two separate loops. Another loop controller with simple PID control strategy is aimed to stabilize body acceleration. This provides a ride control that separates the vehicle body from unwanted pitch and roll moment caused by road disturbance. The outer loop utilizes a PID controller to provide a ride control that separates the vehicle body from pitch and roll moment caused by road disturbance. Meanwhile, the inner loop controller is developed with Skyhook control strategy which provides imaginary damper to the vehicle model to improve damping characteristic of the suspension system. The inner loop controller will provide the desired damping force for the semi active damper to dissipate any unwanted motion. For better compatibility for both controllers a decoupling transformation model is positioned between the inner and outer loop controllers. This will ensure that the control output from the outer loop to be compatible with seven DOF vehicle ride model. The detailed derivation and development of the decoupling transformation module will be discussed in next section. The proposed control structure is shown in Figure 3.

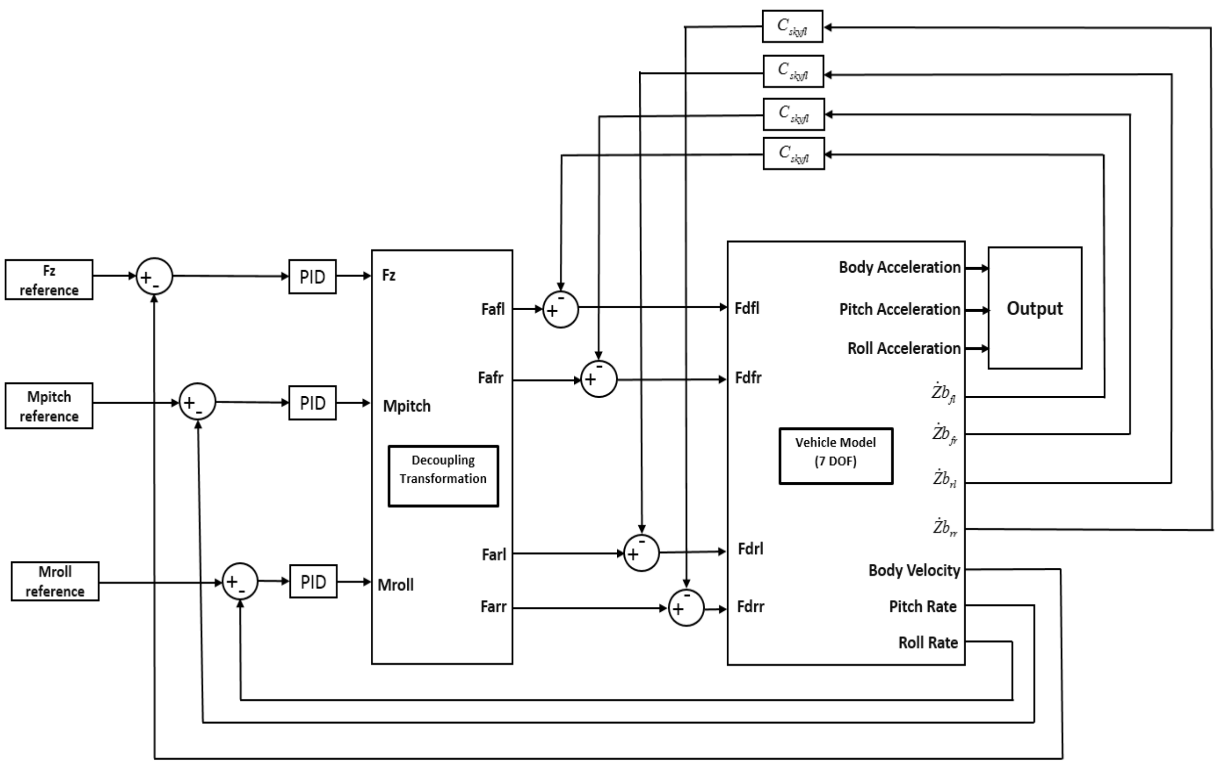

Figure 3. Hybrid control structure for semi active suspension system without optimization

2.3 Decoupling Transformation and PID Controller

Decoupling transformation is a subsystem that requires further understanding of vehicle dynamic system (Ahmad et al., 2010). The output of outer loop controller is used to stabilize body bounce force F_z and moment to stabilize pitch moment, M_θ and roll moment, M_φ. Meanwhile, the output of decoupling transformation model provide the desired actuator forces for inner loop controller which will provide the ideal damper force to stabilize the vehicle model. According to Equation (1) to Equation (3) equivalent bounce force for sprung mass F_z, moment for pitch M_θ, and moment for roll M_φ can be defined by;

$$F_z = F_{dfl} + F_{dfr} + F_{drl} + F_{drr} \tag{8}$$

$$M_\theta = -F_{dfl}.l_F - F_{dfr}.l_F + F_{drl}.l_R + F_{drr}.l_R \tag{9}$$

$$M_\varphi = F_{dfl}\left(\frac{w}{2}\right) - F_{dfr}\left(\frac{w}{2}\right) + F_{drl}\left(\frac{w}{2}\right) - F_{drr}\left(\frac{w}{2}\right) \tag{10}$$

F_{dfl} ,F_{dfr} ,F_{drl} ,F_{drr} in decoupling transformation model are the desired forces produced by the outer loop controller in right front, left front, left rear and right rear respectively. This will produce an ideal targeted force for semi active suspension system in seven DOF ride model. Equation (8) to Equation (10) can be rearranged in matrix form as following.

$$\begin{bmatrix} F_z(t) \\ M_\theta(t) \\ M_\varphi(t) \end{bmatrix} = \begin{bmatrix} 1 & 1 & 1 & 1 \\ -l_F & -l_F & l_R & l_R \\ \frac{w}{2} & -\frac{w}{2} & \frac{w}{2} & -\frac{w}{2} \end{bmatrix} \begin{bmatrix} F_{dfl} \\ F_{dfr} \\ F_{drl} \\ F_{drr} \end{bmatrix} \tag{11}$$

A linear equations system y = **Cx**, if $\mathbf{C} \in \Re^{mxm}$ contains full row rank, then there exists a right inverse C^{-1} such that $C^{-1}C = I^{mxm}$. The right inverse can be computed using $C^{-1} = C^T\left(CC^T\right)^{-1}$. Thus, the inverse relationship of Equation (11) can be expressed as:

$$\begin{bmatrix} F_{dfl} \\ F_{dfr} \\ F_{drl} \\ F_{drr} \end{bmatrix} = \begin{bmatrix} \frac{l_R}{2(l_R+l_F)} & -\frac{1}{2(l_R+l_F)} & \frac{1}{2W} \\ \frac{l_R}{2(l_R+l_F)} & -\frac{1}{2(l_R+l_F)} & -\frac{1}{2W} \\ \frac{l_F}{2(l_R+l_F)} & \frac{1}{2(l_R+l_F)} & \frac{1}{2W} \\ \frac{l_F}{2(l_R+l_F)} & \frac{1}{2(l_R+l_F)} & -\frac{1}{2W} \end{bmatrix} \begin{bmatrix} F_z \\ M_\theta \\ M_\varphi \end{bmatrix} \tag{12}$$

This equation was developed as a decoupling transformation subsystem as shown in Figure 3. For the outer loop controller, a simple PID controller is used for suppressing body velocity, pitch rate and roll rate. Parameters for simple PID controller were chosen by trial and error and can be summarized in Table 1.

Table 1. PID Controller Parameter

PID Controller	**K_P**	**K_I**	**K_D**
Body velocity, $\ddot{Z}$	200000	1	10
Body roll rate, $\ddot{\varphi}$	600000	1	100
Body pitch rate, $\ddot{\theta}$	150000	10	100

2.4 Skyhook Controller

For the inner loop controller, Skyhook controller is proposed to provide imaginary damper to the semi-active suspension system as shown in Figure 4. The imaginary damper is fixed between the sprung mass, M_s and virtual inertial space (Yu et al., 2011). The ideal equation of skyhook damping force, F_{sky} is given by;

$$F_{sky} = -C_{sky}\,\dot{x}_1 \tag{13}$$

In theory, the imaginary damper will be used to determine the desired damping force required to stabilize the vertical motion. In this study, this virtual force will be realized by the semi active damper located between sprung and unsprung masses. Therefore, Skyhook gain, C_{sky} can be optimized by optimizing the damping coefficient of the armored vehicle's damper.

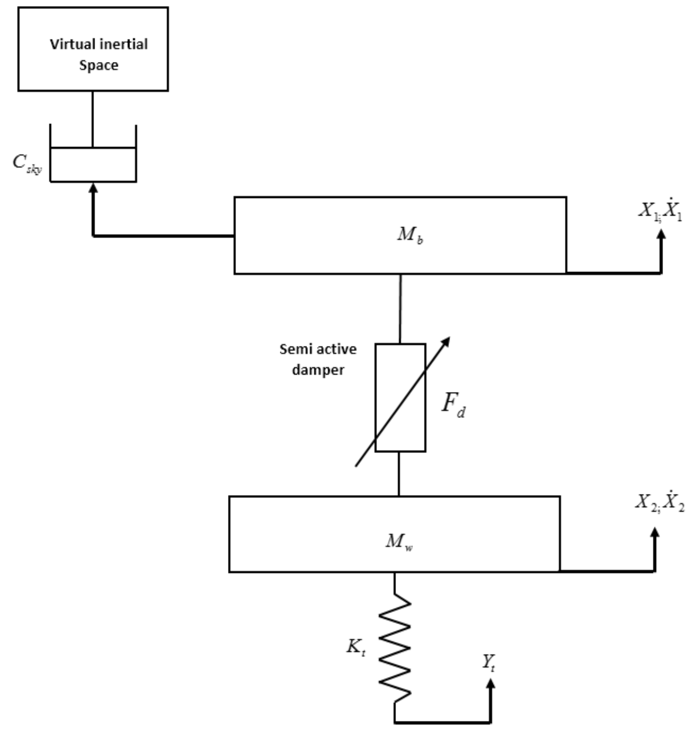

Figure 4. Skyhook equivalent force

From Figure 4, damper force of the semi-active absorber, F_d can be defined by

$$F_d = -C_{sa}(\dot{x}_2 - \dot{x}_1) \tag{14}$$

Since the skyhook damper model and semi active damper model are equivalent, the following equation can be derived:

$$F_{sky} = -C_{sky}\dot{x}_1 = -C_{sa}(\dot{x}_2 - \dot{x}_1) = F_d \tag{15}$$

Parameters for skyhook controller is chosen by trial and error and can be summarized in Table 2.

Table 2. Skyhook controller parameter

SKYHOOK Controller	Value (N/m^{-1})
SKYHOOK1(C_{skyRR})	20000
SKYHOOK2(C_{skyRL})	20000
SKYHOOK3(C_{skyFR})	25000
SKYHOOK3(C_{skyFL})	25000

2.5 Particle Swarm Optimization (PSO) for Hybrid Controller Parameters

The Hybrid control structure must be optimized by optimization method to provide an optimum value for the Skyhook gain. Optimization method used in this study is a Particle Swarm Optimization (PSO) method. PSO is an optimization strategy that mimics the behavior of various agents moving in swarm. Each agent carries its own fitness level which will determine its next position and velocity of travel. The particle with best fitness will be chosen to represent the solution to optimization problem. As a swarm, each particle then will exchange information about their position, velocity and fitness and the behavior of the swarm will be influenced to increase the probability of particle migration to the region of high fitness. PSO is often chosen as an optimization strategy due to its simple operation and efficient algorithm.

After PSO chooses parameter for the optimum solution, it will multiply the parameter by uniform random term to prevent premature convergence. Particles which are the individuals that formed at the beginning of PSO process will remain fully function till the best solution is found. On the other hand, the process for optimization continues until either algorithm achieves desired result or acceptable solution cannot be found within computational limit. There are two factors that fluent the movement of particle which are global particle to particle best solution and local particle iteration to iteration best solution. These two factors will determine the direction and amount of movement resulting from particle velocity.

The PSO defines position for X_i each particle in the D-dimensional space as

$$X_i = (X_{i1}, X_{i2}, .\dots\dots, X_{iD}) \tag{16}$$

where the subscript 'i_{th}' represents the particle number and the second subscript is the dimension, which corresponds to the number of parameters defining the solution. The memory of the previous best position is represented as,

$$p_i = (p_{i1}, p_{i2}, .\dots\dots, p_{iD}) \tag{17}$$

For each i_{th} particle, Velocity, v_i for each dimension is independently established as;

$$v_i = (v_{i1}, v_{i2}, .\ldots\ldots, v_{iD}) \tag{18}$$

After each iteration, the velocity term is updated and the particle is moved with some randomness in the direction of its own best position, p_{best}, and the global best position, g_{best} based on its own velocity in all dimensions. This is apparent in the velocity update equation, given by;

$$v_{id}^{(t+1)} = w \times v_{id}^{(t)} + c \times U[0,1] \times (p_{id}^{(t)} - X_{id}^{(t)}) + s \times U[0,1] \times (p_{gd}^{(t)} - X_{id}^{(t)}) \tag{19}$$

The new position is then according to the velocity from (19) ;

$$X_{id}^{(t+1)} = X_{id}^{(t)} + v_{id}^{(t)} \tag{20}$$

where,

$U\,[0,1]$ = samples a uniform random distribution from 0 to 1
t = relative time index
c = weights trading off the impact of the local best solutions
s = weights trading off the impact of the global best solutions
w = weight of inertia impact for each particle

The particle swarm optimization algorithm is highly efficient in searching complex and continuous solution landscapes. The PSO can also be implemented as a parallel algorithm by improving its efficiency for real-time applications. In addition, The particles can be split up among multiple processors and then the global best solution is shared among the particles.

In this study, PSO is used to optimize the value of C_{sky} for each wheel respectively. There are 4 values of C_{sky} corresponding to four input variables to be optimized. This means that the swarm particles will have four dimensions each. Position for each particle, X_i corresponds to values of the four input variables. These values will be applied on the controller model which will evaluate body, pitch and roll acceleration. These three responses will be formulated to be the objective functions for the optimization problems follows:

Fitness function, $J(X_i) = \sqrt{\ddot{Z}^2 + \ddot{\theta}^2 + \ddot{\varphi}^2}$ (21)

Here, $\ddot{Z}$, $\ddot{\theta}$, and $\ddot{\varphi}$ are the RMS values for body, pitch and roll acceleration respectively. The particle with the best fitness will be chosen and compared with the personal best record and global best record. Position for the best particle will be saved for next iterations.

To summarize, Table 3 lists the main parameters values used in the PSO optimization and Figure 5 shows the algorithm for Particle Swarm Optimization to optimize Skyhook controller parameters for hybrid control structure.

Table 3. PSO parameter to optimize Skyhook controller

PSO Parameter	**Value**
X_i	5
d	4
k	10
c	1.42
s	1.42
w	0.9

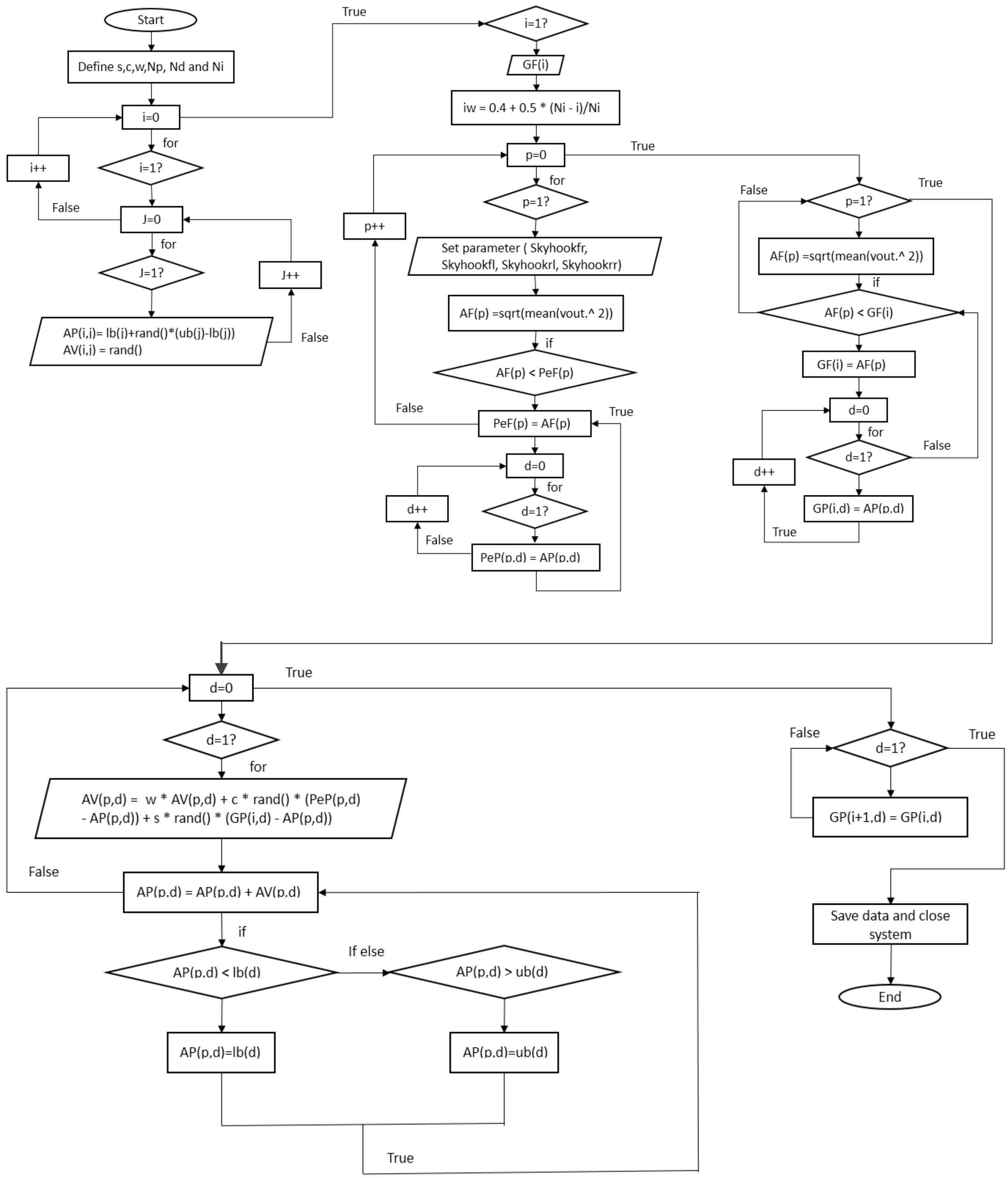

Figure 5. PSO algorithm to optimize Skyhook controller

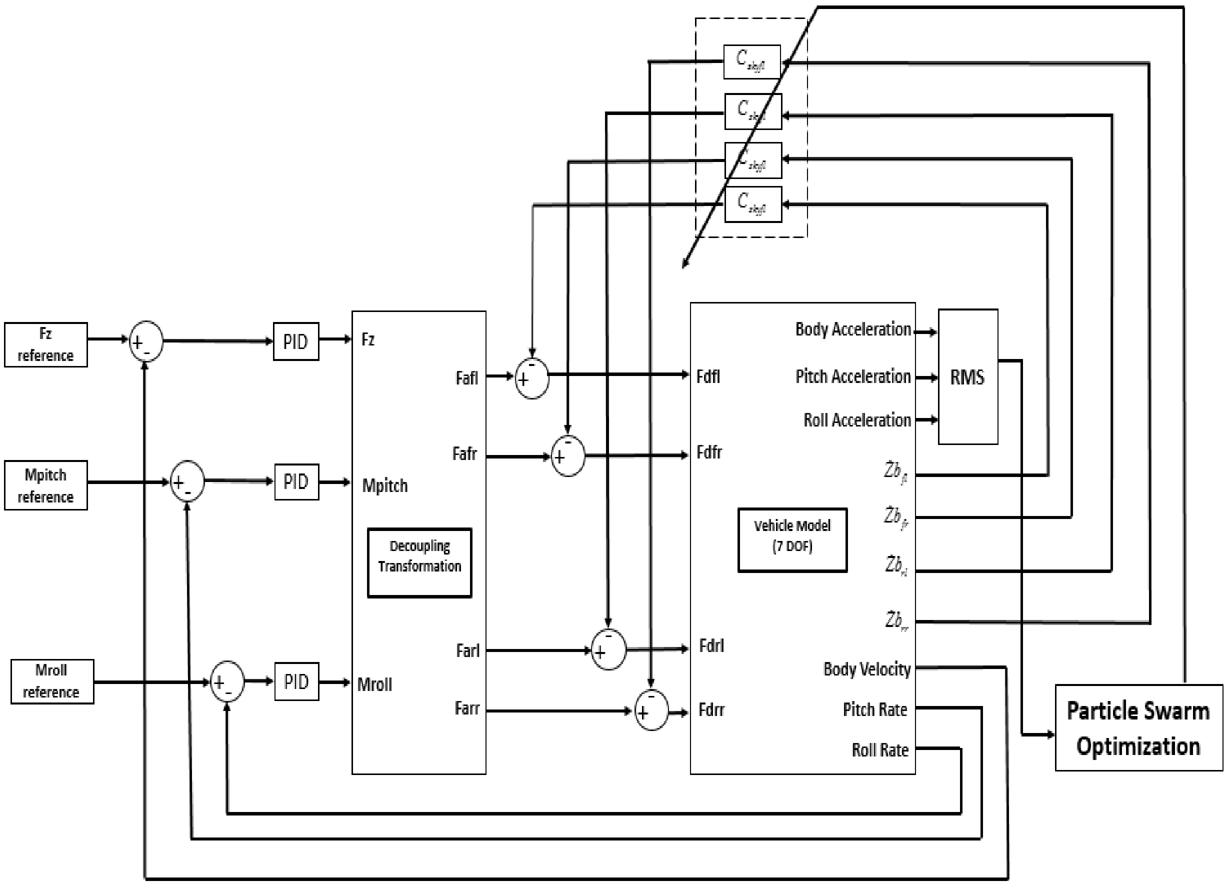

Figure 6. Hybrid control structure for semi active suspension system optimized by Particle Swarm Optimization algorithm

Figure 6 shows the overall hybrid control structure with PSO optimization. As shown in the Figure 6, the hybrid control structure for Stability Augmentation System (SAS) uses PID and Skyhook controller. The outer controller which utilized PID controller provides a ride control that separates vehicle body from roll moment and pitch moment that caused by road disturbance by stabilizing body acceleration, body pitch and body roll response of vehicle body. Meanwhile, Skyhook controller will provide imaginary damper to the vehicle model to improve the damping characteristics of vehicle suspension system. Skyhook controller will provide the desired damping force for the semi active suspension system to remove any unwanted motion. However without an optimization value of Skyhook gain for Skyhook controller, the performance of vehicle model will not be at the best stage. The purpose of Particle Swarm Optimization is to optimize and determine the optimum values for Skyhook gain in Skyhook controller to enhance the ride and stability performance of vehicle model.

3.0 PERFORMANCE EVALUATION

The function of the nonlinear mathematical model of seven DOF ride model is to simulate the dynamic characteristic in observing the vertical performance of the vehicle model in terms of its body acceleration, body pitch acceleration, and body roll acceleration responses. Simulation for the proposed hybrid control strategy was carried out by using a ride over bump test within MATLAB/SIMULINK software. In real life application, ride over bump will cause roll moment and pitch moment that will cause discomfort to the soldier travelling in the armored vehicles. Besides, the extreme road profile faced by armored vehicle during operation also may cause pitch and roll moment that may cause wheels to lose contact with the road surface. Consequently, this will lead to fatal accidents. From the simulation, the response of vehicle body acceleration, body pitch acceleration and body roll acceleration were observed in order to improve ride quality and performance of the armored vehicle. The ride over bump test was chosen since this is the commonly road condition faced in the armored vehicle during operation. A sine wave was generated as road input to seven DOF vehicle ride model with the amplitude of 0.1 m, frequency of 1 rad/sec and for different phase at each wheels as shown in Table 4. With a fixed step size of 0.01 second, the simulation was executed for 10 seconds by using Bogacki–Shampine solver. HMMWV was selected as a benchmark for vehicle simulation model due to its similar characteristics to the armored vehicle.

Table 4: Phase for road input at each tires

Tire	**Phase**
Front Left	0
Front Right	Pi/4
Rear Left	Pi/2
Rear Right	Pi/3

The parameter for seven DOF vehicle ride model are as shown in Table 5. The values were manipulated within acceptable range value to make sure the response from model simulation can be verified with the output response from the CARSIM software response as reported in previous study (Amin et al., 2015). In the hybrid controller design, reference value for F_z, M_{pitch} and M_{roll} are set to be zero. In this study, the ride performance of vehicle model will be evaluated against passive vehicle model, vehicle model with simple PID control structure (no inner loop controller), with vehicle model hybrid control structure and vehicle model with hybrid control structure, optimized by Particle Swarm Optimization (PSO) algorithm. In this study, the proposed PSO optimized hybrid controller performance will be evaluated by comparing the ride performance of the vehicle model with passive suspension, semi active suspension with outer loop PID controller (no inner loop), and hybrid control structure without PSO.

Table 5. Seven DOF ride model parameter based on HMMWV

Parameter	**Value**
Base front	1.07 m
Base rear	2.232 m
K_{sfl}, K_{sfr}, K_{srl}, K_{srr}	35000 N/m
C_{sfl}, C_{sfr}, C_{srl}, C_{srr}	3000 Ns/m
K_{tfl}, K_{tfr}, K_{trl}, K_{trr}	450000 N/m
Inertia pitch	4331.6 kg.m^2
Inertia roll	1243.1 kg.m^2
Sprung mass	2210 kg
Mass wheel	125 kg
Wheel base	1.9 m

3.1 Simulation Results

The performance of the hybrid control structure with Particle Swarm Optimization (PSO) was evaluated in time domain simulation. The responses for body acceleration, body pitch and body roll acceleration will be observed to investigate its effectiveness in improving ride performance of the seven DOF vehicle ride model of armored vehicle.

The body acceleration response for hybrid control structure optimized by PSO improved drastically than that of hybrid control structure without optimization, followed by simple PID control structure and lastly, passive suspension performance. As shown in Figure 7, the amplitude of body acceleration responses for PSO optimized hybrid controller was the lowest than the other control structures during the transient state response. In a steady state response, the response of hybrid control structure optimized by PSO performs better than other controllers. From the simulation, it takes about 1.56 seconds for the body acceleration response of hybrid control structure optimized by PSO, to enter steady state. Eventhough the responses of all control structure show better performance than passive suspension, there are some chattering visible on the response at transient state. However, the chattering can be neglected due to the significantly small value (peak to peak) and does not affect the ride performance of vehicle model. The percentage maximum overshoot reduction for hybrid control structure optimized by PSO was reduced by 92.01%, followed by hybrid control structure without optimization 90.15% and lastly simple PID control structure 86.51% compares to passive suspension. Meanwhile for the improvement, Root Mean Square (RMS) average percentage of reduction for body acceleration response was shown in Table 6.

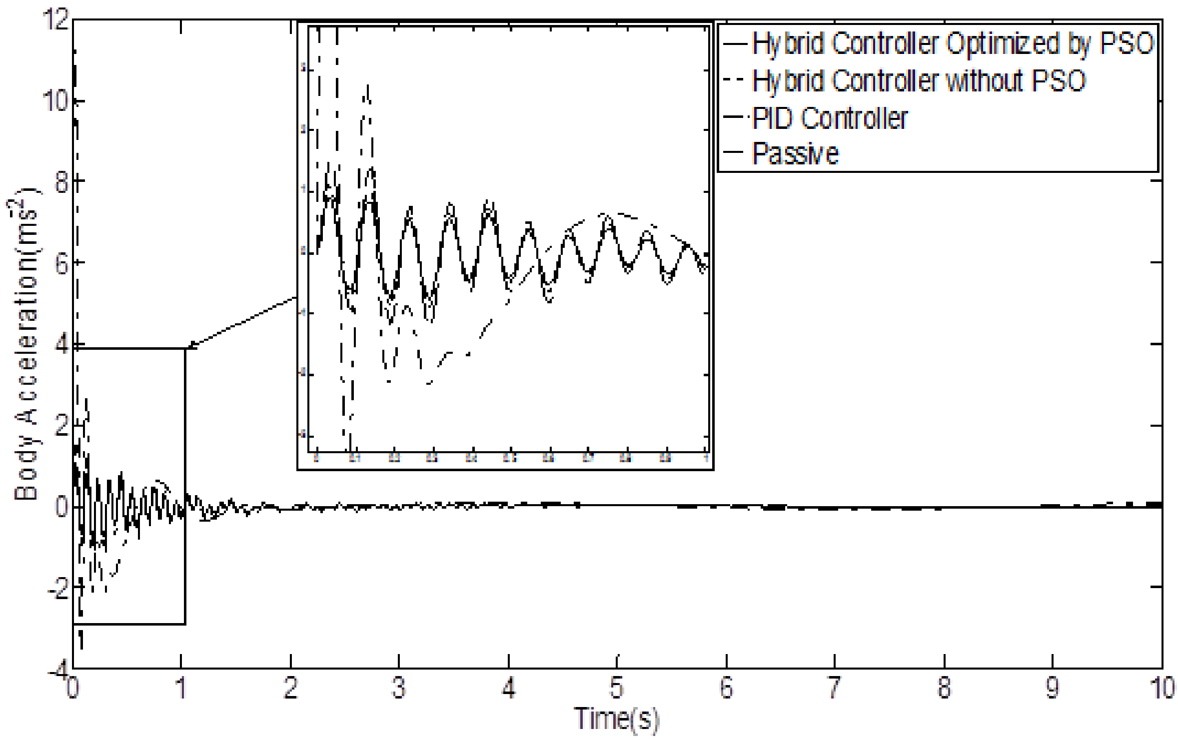

Figure 7. Body acceleration response for different control strategies

Table 6. RMS percentage of reduction for body acceleration response

Control strategies	**RMS percentage of reduction (%)**
Simple PID controller	26.06
Hybrid controller without optimization	48.80
Hybrid controller optimize by PSO	59.02

Observing body pitch acceleration response as shown in Figure 8, it was shown that Hybrid control structure optimized by PSO algorithm provide a better result in reducing pitch acceleration of the seven DOF vehicle ride model of armored vehicle. It can be seen that the Hybrid control structure without optimization shows better performance for body pitch acceleration response than PID control structure. From Figure 8, the amplitudes of body pitch acceleration response for Hybrid control structure optimized by PSO was lower than Hybrid control structure without optimization followed by simple PID control structure and passive suspension. From the simulation result, body pitch acceleration response it takes 1.66 seconds from to enter steady state response from transient state. In transient state response, there are some chattering visible. However, the chattering were significantly small to be considered and does not affect the ride performance of vehicle model. Meanwhile for the improvement, peak to peak percentage of reduction was shown in Table 7.

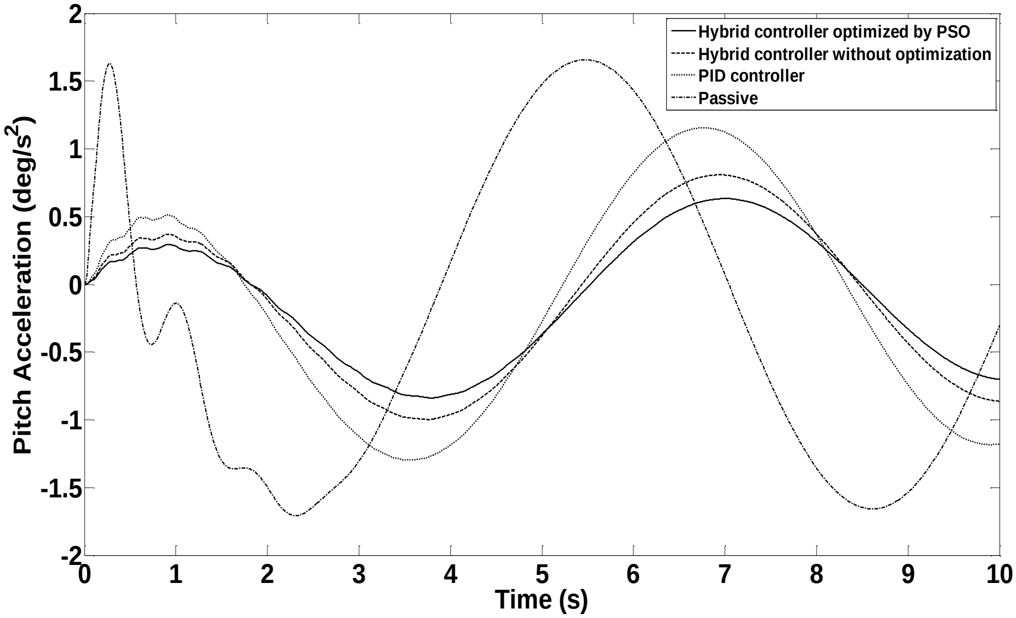

Figure 8. Pitch acceleration response for different control strategies

Table 7. Peak to peak percentage of reduction for pitch acceleration response

Control strategies	**Peak to peak percentage of reduction (%)**
Simple PID controller	29.44
Hybrid controller without optimization	49.51
Hybrid controller optimize by PSO	59.62

In Figure 9 body roll acceleration responses were presented. It was shown that PSO optimized hybrid controller has shown a better performance than hybrid control structure without optimization followed by simple PID control structure and passive seven DOF vehicle ride model. From Figure 9, the response of body roll acceleration takes about 2.22 seconds from transient state to steady state phase response. In transient state response, there are some chattering visible on the response. However, the chattering was significantly small to be considered and does not affect the ride performance of vehicle model. In steady state, the amplitudes of body roll acceleration response for hybrid control structure optimized by PSO was lower than other control structure and passive seven DOF vehicle ride model. Meanwhile for the improvement, peak to peak percentage reduction was shown in Table 8.

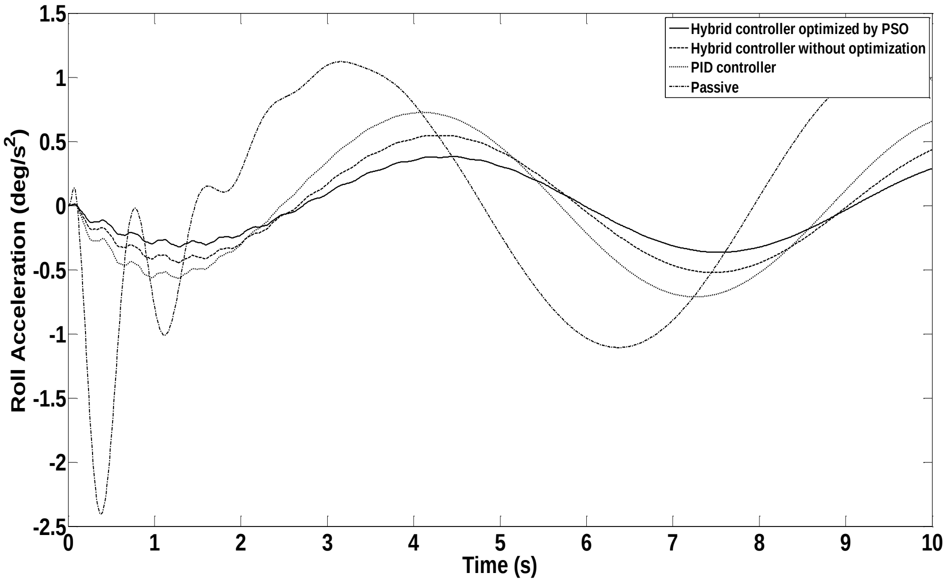

Figure 9. Roll acceleration response for different control strategies

Table 8. Peak to peak percentage of reduction for roll acceleration response

Control strategies	**Peak to peak percentage of reduction (%)**
Simple PID controller	35.88
Hybrid controller without optimization	53.29
Hybrid controller optimize by PSO	66.56

From the three performance criteria reported before, two observations can be stated:

i. The proposed Hybrid controller perform better than simple PID controller in improving ride performance; and
ii. The PSO implementation has managed to improve the performance of the Hybrid controller.

4.0 CONCLUSION

In conclusion, it is clearly shown that the hybrid control structure is capable to improve the body acceleration, body pitch acceleration and body roll acceleration responses better than PID control structure and passive suspension system of seven DOF vehicle ride model. Moreover, hybrid control structure optimized by PSO algorithm gives better improvement for ride performance than hybrid control structure without optimization. Due to these improvements, the ride performance and stability of the armored vehicle improved drastically by using the proposed control structure. In real life application, ride and handling performance during combat training or in battlefield can be improved by isolating the armored vehicle from vibration due to road disturbance and extreme road profiles. This will improve stability, provide comfort to the soldier traveling in the armored vehicle and maintaining contact between wheel and road surface. Hence, fatal accident that killed soldier may be prevented, and the cost of repairing the armored vehicle that involved in an accident due to poor maneuvering can be reduced.

ACKNOWLEDGEMENT

This work is part of the research project entitled Robust Stabilization of Armored Vehicle Firing Dynamic Using Active Front Wheel Steering System. This research is fully supported by LRGS grant (No. LRGS/B-U/2013/UPNM/DEFENSE & SECURITY – P1) led by Dr. Khisbullah Hudha. The authors would like to thank the Malaysian Ministry of Science, Technology and Innovation (MOSTI), Malaysian Ministry of Education and Universiti Pertahanan Nasional Malaysia (UPNM) for the continuous support in this research work.

REFFERENCES

Abu Bakar, S. A., Jamaluddin, H., Rahman, R. A., Samin, P. M., & Hudha, K. (2008). Vehicle ride performance with semi-active suspension system using modified skyhook algorithm and current generator model. *International Journal of Vehicle Autonomous Systems, 6*(3-4), 197-221.

Ahmad, F., Hudha, K. , & Jamaluddin, H., (2010), Adaptive PID Control With Pitch Moment Rejection For Reducing Unwanted Vehicle Motion In Longitudinal Direction, *Journal of Mechanical Engineering and Technology*, 2(2):27-64.

Dhir, A. & Sankar ,S., (1997). Analytical wheel models for ride dynamic simulation of off-road tracked vehicles. *Vehicle System Dynamics* 27(1): 37-63.

Amin, M., Hudha, K., Kadir, Z. A., & Amer, N. H. (2015). Skyhook control for 7 DOF ride model of armored vehicle due to road disturbance. 10th Asian IEEE Control Conference (ASCC). 1-5.

Chen, Y., Wang, Z. L., Qiu, J., & Huang, H. Z. (2012). Hybrid fuzzy skyhook surface control using multi-objective microgenetic algorithm for semi-active vehicle suspension system ride comfort stability analysis. *Journal of Dynamic Systems, Measurement, and Control*, *134*(4): 041003.

Hayes, R. J., Beno, J. H., Weeks, D. A., Guenin, A. M., Mock, J. R., Worthington, M. S., & Lippert, D. (2005). Design and Testing of an Active Suspension System for a 2-1/2 Ton Military Truck. SAE Technical Paper, 2005-01-1715.

Hoogterp, F., Saxon, N., & Schihl, P. (1993). Semiactive suspension for military vehicles. SAE Technical Paper 930847.

Hosseinloo, A. H., Vahdati, N., & Yap, F. F. (2012). Performance of spade-less wheeled military vehicles with passive and semi-active suspensions during mortar firing. *Vehicle System Dynamics*, *50*(10), 1515-1537.

Hudha, K., Jamaluddin, H., Samin, P. M., & Rahman, R. A. (2005). Effects of control techniques and damper constraint on the performance of a semi-active magnetorheological damper. *International Journal of Vehicle Autonomous Systems*, *3*(2-4), 230-252.

Hudha, K., Jamaluddin, H., & Samin, P. M. (2008). Disturbance rejection control of a light armoured vehicle using stability augmentation based active suspension system. *International Journal of Heavy Vehicle Systems*, *15*(2-4), 152-169.

Liang, Y. J., & Wu, S. L. (2013). Optimal vibration control for tracked vehicle suspension systems. *Mathematical Problems in Engineering*, 2013: 178354.

Miller, L. R., & Nobles, C. M. (1988). The design and development of a semi-active suspension for a military tank. SAE Technical Paper 881133.

Trikande, M. W., Jagirdar, V. V., & Sujithkumar, M. (2014). Modelling and Comparison of Semi-Active Control Logics for Suspension System of 8x8 Armoured Multi-Role Military Vehicle. *Applied Mechanics and Materials*, 592: 2165-2178.

Setiawan, J. D., Safarudin, M., & Singh, A. (2009). Modeling, simulation and validation of 14 DOF full vehicle model. IEEE International Conference on Instrumentation, Communications, Information Technology, and Biomedical Engineering (ICICI-BME), 1-6.

Uddin, N., (2009). Stochastic Optimal Preview Control for Active Suspension Systems of a Full Tracked Vehicle Model Stochastic Optimal Preview Control for Active Suspension Systems of a Full Tracked Vehicle Model. MSc Thesis. Gyeongsang National University.

Weeks, D. A., Bresie, D. A., Beno, J. H., & Guenin, A. M. (1999). The design of an electromagnetic linear actuator for an active suspension. SAE Technical Paper, 1999-01-0730.

Yu, Z. X., Chen, Z., & Li, J. H. (2011). Simulation of Control Strategy for Automotive Semi-active MRF Dampers. IEEE International Conference on Information Technology, Computer Engineering and Management Sciences (ICM), (3):96-99.